

Article

Chinese Colorless HPHT Synthetic Diamond Inclusion Features and Identification

Ying Ma¹, Zhili Qiu^{2,*}, Xiaoqin Deng², Ting Ding¹, Huihuang Li¹, Taijin Lu³, Zhonghua Song³, Wenfang Zhu¹ and Jinlin Wu¹

¹ National Gemstone Testing Center Shenzhen Lab. Company Ltd., ShenZhen 518000, China

² School of Earth Sciences and Engineering, Sun Yat-sen University, GuangZhou 510275, China

³ Jewelry Technology Administrative Center, Ministry of Natural Resources, Beijing 100013, China

* Correspondence: qiuzhili@mail.sysu.edu.cn; Tel.: +86-138-2600-8304

Abstract: Chinese HPHT diamonds have improved dramatically in recent years. However, this brings a challenge in identifying type IIa colorless diamonds. In this study, eleven HPHT and three natural, colorless, gem-quality IIa diamonds were analyzed using magnified observation, Raman, PL and chemical element analysis. The results show that only HPHT samples possessed kite-like inclusions and lichenoid inclusions, as verified by their complex Raman spectra (100–750 cm⁻¹). Through PL mapping, HPHT and natural IIa diamonds were distinguished by their growth environments, which were reflected by PL peaks at 503, 505, 575, 637, 693, 694 and 737 nm. The chemical components of HPHT IIa diamond carbide inclusions are mainly Fe, Co, Ni and Mn, but those of Natural IIa are mainly Fe and Ni. As a result, the chemical components can be used to distinguish a natural colorless IIa diamond from a synthetic diamond.

Keywords: HPHT diamond; inclusion; PL mapping; chemical components



Citation: Ma, Y.; Qiu, Z.; Deng, X.; Ding, T.; Li, H.; Lu, T.; Song, Z.; Zhu, W.; Wu, J. Chinese Colorless HPHT Synthetic Diamond Inclusion Features and Identification. *Crystals* **2022**, *12*, 1266. <https://doi.org/10.3390/cryst12091266>

Academic Editor: Giuseppe Prestopino

Received: 10 August 2022

Accepted: 30 August 2022

Published: 6 September 2022

Publisher's Note: MDPI stays neutral with regard to jurisdictional claims in published maps and institutional affiliations.



Copyright: © 2022 by the authors. Licensee MDPI, Basel, Switzerland. This article is an open access article distributed under the terms and conditions of the Creative Commons Attribution (CC BY) license (<https://creativecommons.org/licenses/by/4.0/>).

1. Introduction

HPHT synthetic diamonds are fundamental for high-pressure research (Crystals 2021, 11, 1185). Thanks to advancements in experimental techniques and computer simulations, the rate of new, important discoveries has significantly increased. Chinese HPHT synthetic diamonds have improved dramatically since the first was produced in China in 1963 [1–3]. After 2016, manufacturers began to produce high-quality IIa diamonds which have been made available in the Chinese jewelry market in large quantities [2–5] (see Figure 1). Nevertheless, HPHT synthetic diamonds are often sold as natural diamonds, or natural diamond parcels are intentionally mixed with HPHT synthetics [4]. There have been reports of cases of fraud in the global diamond business [2–4]. Therefore, there is a demand for distinguishing between natural and synthetic diamonds in the jewelry market.

Luminescence is currently used to identify IIa colorless diamonds. DeBeers company developed the DiamondView fluorescence imaging microscope using an ultra-shortwave excitation of 225 nm in the 1990s to distinguish HPHT-growth diamonds from natural diamonds [6]. They have developed a variety of methods since then, including cathodoluminescence (CL) images, X-ray images, PL spectrums, IR spectrums and inclusion tests [2,3,7,8]. DiamondView fluorescence imaging, PL spectrums and IR spectrums are the most commonly used methods for identifying diamonds. However, under DiamondView fluorescence imaging, many synthetic diamonds have a similar fluorescence color or IR spectrum to natural diamonds, especially IIa diamonds. There are also difficulties distinguishing between natural and synthetic diamonds using only fluorescence imaging, PL and IR spectrums with the progress of synthetic diamond technology. Gemologists face a challenge in identifying IIa colorless diamonds.

Inclusion characteristics, which reflect the diamond's formation environment, are also necessary for identifying diamonds [3,5]. This article discusses eleven HPHT-growth IIa

colorless diamonds from three producers (HH-HuangHe, J-HuaJing and Z-ZhongNan) and three natural ones from natural primary diamond deposits (Guizhou). With the addition of previous corresponding research results, this article reports that special inclusions, their Raman features and chemical components are useful for identifying natural diamonds and HPHT synthetic colorless diamonds.



Figure 1. Jewelry made from Chinese HPHT synthetic diamonds (weights ranging from 0.01 to 5.00 ct), 2019. Images courtesy of two companies (Zhengzhou Sino-Crystal Diamond Co., Ltd. Shenzhen Multi-Win Business Co., Ltd.-VCK growth Diamond, China).

2. Materials and methods

2.1. Materials

In this study, 14 samples were tested, including 11 HPHT type IIa colorless diamonds from three Chinese factories (HH, J, Z) and three natural type IIa colorless diamonds selected from the primary diamond mine in Guizhou (China), which are presented in Table 1 and Figure 2. Eleven HPHT type IIa colorless diamonds were cut and polished to expose inclusions near the surface, with the cuts oriented by the {111}, {100} and {110} planes. We also cut the three rough Guizhou diamonds with irregular shapes into plates. We cleaned all of the plates without inclusions on the diamond face in acetic acid for 1 h at 100 °C. The detailed inclusions and PL peak characteristics of these samples are described in Table 1.

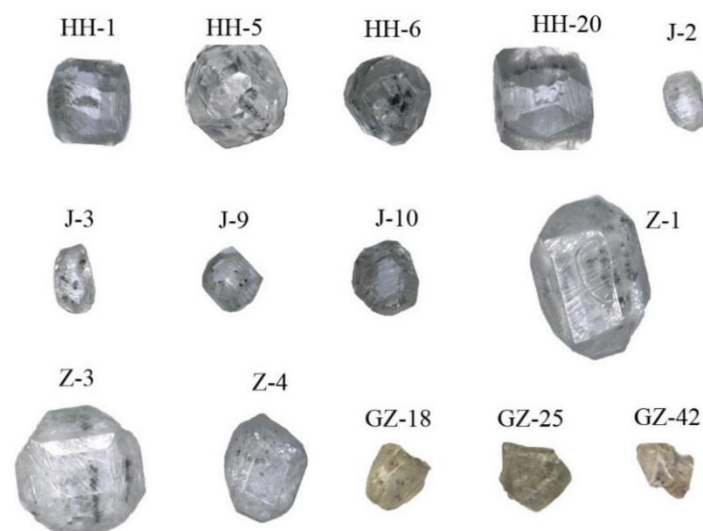


Figure 2. Diamond samples.

Table 1. Characteristic of Chinese HPHT synthetic diamonds in recent years.

Sample NO.	Color/Type	Weight/ct	Shape	Inclusion Properties	Inclusion Assemblage	Emission Peaks	Origin
HH-1	Colorless/Ia	0.23	Hexoctahedron	Tiny point-like inclusions, less than 1 μm	-	-	HuangHe
HH-5	Colorless/Ia	0.35	Hexoctahedron	Block-shaped, rod-like, greater than 150 μm	Carbide, magnetite, hematite, sulfide, graphite, methane	416, 509, 533, 538, 693, 694, 883, 884 nm	HuangHe
HH-6	Colorless/Ia	0.20	Hexoctahedron	Water-drop, tiny point-like inclusions, less than 1 μm	Carbide, graphite	693, 694, 883, 884 nm	HuangHe
HH-20	Colorless/Ia	0.38	Hexoctahedron	Tiny point-like inclusion distributed along the edge of a crystal, less than 1 μm	-	883, 884 nm	HuangHe
J-2	Colorless/Ia	0.07	Hexoctahedron	Kite-like, tubular (cone like) inclusions (1~10 μm)	-	505, 737, 883 nm	HuaJing
J-3	Colorless/Ia	0.06	Hexoctahedron	Disc shape, point-like inclusions (1~90 μm)	Carbide, graphite	505, 737, 877 nm	HuaJing
J-20	Colorless/Ia	0.05	Hexoctahedron	Point-like inclusions (1~50 μm)	-	575, 637, 737 nm	HuaJing
J-10	Colorless/Ia	0.15	Hexoctahedron	Tiny point-like inclusions, less than 1 μm , Tubular (cone like) inclusions	-	737 nm	HuaJing
Z-2	Colorless/Ia	1.02	Hexoctahedron	Rod like inclusions (1~5 μm)	Carbide, graphite, methane	484, 489, 491, 883, 884 nm	ZhongNan
Z-3	Colorless/Ia	1.00	Hexoctahedron	Lichenoid (tree-like) inclusions, point-like inclusions (1~80 μm)	Metal alloy, methane	484, 489, 507, 883, 884 nm	ZhongNan
Z-4	Colorless/Ia	0.50	Hexoctahedron	Water-drop, point-like inclusions (1~50 μm)	Metal alloy, carbide, graphite	693, 694, 883, 884 nm	ZhongNan
GZ-18	Colorless/Ia	0.12	Irregular	Irregular inclusions	Graphite	491, 496, 503, 505, 536, 575, 579, 637, 612, 676, 710, 741 nm	GuiZhou
GZ-25	Colorless/Ia	0.17	Irregular		-	406, 415, 491, 496, 741 nm	GuiZhou
GZ-42	Colorless/Ia	0.10	Irregular		-	406, 415, 491, 496, 741, 945 nm	GuiZhou

2.2. Methods

Photomicrographs of samples were tested at the School of Earth Sciences and Engineering (SESE), Sun Yat-sen University, using digital (VHX-5000, Keyence, Japan) and polarizing (BX51, Olympus, Japan) microscopic image technology.

A Renishaw inVia Raman micro-spectrometer was used to collect Raman and photoluminescence (PL) spectra with four laser excitations (325, 473, 532 and 785 nm) at room temperature and liquid nitrogen temperature (77 K), at 1 cm^{-1} resolution, for which the laser power was 20 $\text{mw} \times 24\%$ –20 $\text{mw} \times 100\%$.

We performed PL mapping with a Thermo Scientific DXR 2xi Raman imaging microscope equipped with an Olympus optical microscope and an EMCCD detector at Sun Yat-sen University's School of Earth Sciences and Engineering, with an accuracy of 100 nm. We conducted mapping with 455 and 532 nm laser excitation wavelengths. An Olympus 10 \times 0.25 numerical aperture objective lens was used, 1–3 scans were conducted at 2–4 cm^{-1} resolution and the laser power was 10 $\text{mw} \times 20\%$ –10 $\text{mw} \times 100\%$. In addition, the sample was mounted on a liquid-nitrogen-cooled Linkam cold stage for analysis at 123 K. The

data were processed using Thermo Scientific's OMNIC 2xi analysis software package and baseline-corrected peak area profiles were used to produce the observed PL maps.

LA-ICP-MS analyses were performed at the Metallurgical Geology Bureau (MGB) Shandong Bureau, China. The ThermoFisher ThermoX2 laser ablation-inductively coupled plasma-mass spectrometer, coupled with 193 nm LA system was used to analyze trace elements of inclusions in nine samples employed a 10 Hz pulse rate, 30 μm spot size and ablation time of 30–45 s. The US National Institute of Standards and Technology (NIST) standard reference materials 610 and 612 were used for internal calibration. The uncertainty was 1σ .

3. Results and Discussion

3.1. Inclusion Feature

Using microphotographs, inclusions in Chinese type IIa colorless HPHT diamonds appear transparent to opaque, silver or black in color, and range in size from a few hundred to a few microns. Our samples contained rod-like, fine point-like, lichenoid (tree-like), tubular (cone-like), kite-like, pear-shaped and water-drop-shaped inclusions, as shown in Figure 3. All diamonds from the three factories displayed black point-like, rod-like and irregular clusters. Inclusions of a lichenoid (tree-like) nature were mostly found in diamonds from factories Z and HH, see Figure 3. Tubular or kite-like inclusions were only found in factory J, and these were transparent or filled with black materials, reflecting the differences in production methods, see Figure 3J-2. Rod-like, tree-like, pear-shaped and water drop inclusions were metal alloys or carbides, with minor sulfides and phosphides (see Sections 3.2 and 3.3). Some contained graphite coatings and methane jackets (in Raman). As the tubular and kite-like inclusions were too small to analyze, their chemical composition is unknown.

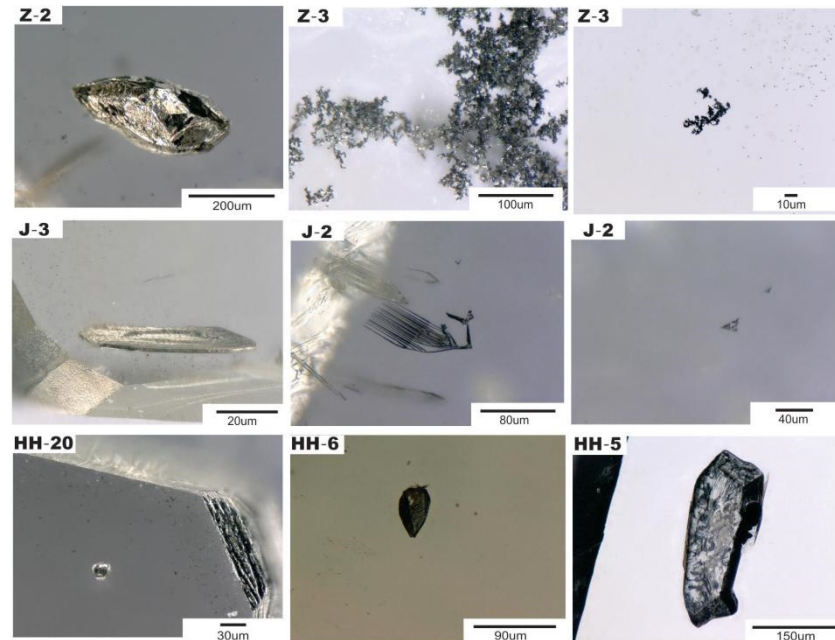


Figure 3. The inclusions in Chinese HPHT synthetic diamonds collected from factories Z, J and HH. **The first row:** Rod-like, lichenoid (tree-like) and fine-point-like inclusions from factory Z, {100}; **The second row:** Disc shape, tubular and kite-like inclusions, {111}, from factory J; **The third row:** Pear or water-drop inclusions, fine-point-like and rod-like inclusions, {111}, from factory HH. These samples were produced in 2017–2020. Photographs by Ying Ma and Xu Ye.

The tubular inclusions (Figure 3J-2) are similar to earlier HPHT diamond cone-like inclusions (the temperature was from 1290 to 1250 $^{\circ}\text{C}$, the pressure was 6 Gpa) from Frumkin Institute of Physical Chemistry and Electrochemistry RAS [9]. Differing from

cone-like inclusions, our samples contained opaque black materials. According to previous research, small-angle grain boundaries (GBs) and associated dislocation bundles decorated with microscopic oxide inclusions are the most plausible explanation for the cone-like defects. Black materials fill the kite-like inclusions in HPHT Ila diamonds (Figure 3J-2). Although there appeared to be networks of planar cracks in natural pink diamond [10], the networks of planar cracks in the natural pink diamonds had multiple planar due to the slip of the crystal plane. However, HPHT synthetic diamonds do not have linear slips in the same way as natural diamonds. The cause of kite-like inclusions appearing in HPHT diamonds is still unclear; however, they can help to distinguish HPHT Ila diamonds from natural diamonds.

3.2. Inclusion Raman Spectroscopy

The Raman method was used to determine inclusions in diamonds using non-destructive testing. In this study, all samples displayed approximately a 1332 cm^{-1} diamond intrinsic Raman line. The three HPHT manufacturers differed. Factory Z samples had a wider HFWT, while J factory samples had a peak at 1400 cm^{-1} , representing graphite D bands. The Raman line of the Guizhou sample showed graphite inclusion and contained the sample's intrinsic peak. Sample differences are not representative of the specific production quality of the three manufacturers and may be caused by sampling. We observed Raman peaks around 2912 cm^{-1} (Figure 4), which corresponds to CH_4 [11,12], see Figure 4J-5. Some HPHT samples contain cohenite inclusions, pear-shaped inclusions and were opaque, silver or black in color, with a graphite coating on the surface, as can be seen in Figures 3 and 4 for HH-20. Furthermore, the Raman spectrum contained many impurity emission peaks, including 4382 cm^{-1} and 4382 cm^{-1} , equal to 692 nm and 693 nm , respectively, which corresponded to Ni (see Figure 4Z-3, right side). Our HPHT sample Z-3 lichenoid inclusions (tree-like inclusions) displayed a complex Raman feature (see Figure 4Z-3, left side). For lichenoid inclusions in HPHT synthetic diamonds, the fit analysis ranged from 100 cm^{-1} to 750 cm^{-1} with software PeakFit V4.12 and Origin 2015, $R^2 > 94\%$. By fitting and dividing the original Raman peak position, Raman emission peaks ($100\text{--}750\text{ cm}^{-1}$) of metal oxide were observed. Ni emission peaks can be seen in the lichenoid inclusion complex's Raman feature at $535\text{--}554\text{ nm}$. The 547 nm (546.6 nm), 540 nm (539.4 nm) and 535 nm (535.2 nm) emission peaks are related to Ni (see Figure 4Z-3, left side). More detailed electronic activities remain to be studied in the future. To the best of the authors' knowledge, Raman spectroscopy of lichenoid inclusions in HPHT Ila diamonds has yet to be found in natural diamonds.

Our research results were compared with those of previous studies to reveal the differences between type Ila natural diamonds and synthetic diamond inclusions (see Table 2). Perovskites and other mineral crystals are common inclusions in natural type Ila diamonds, but amorphous metal compounds, carbides and others can also occur. Inclusions in natural Ila diamonds and HPHT share various similarities, as shown in Table 2. There are inclusions such as metal alloys, carbides, H_2 and CH_4 in both natural and HPHT Ila diamonds, with some inclusions grouped in $\langle 111 \rangle$ chains [13–15]. Since HPHT samples do not undergo as many geological processes as natural diamonds, they do not contain inclusions associated with healed cracks. Crystal minerals appear only in natural Ila diamonds, but not in every diamond. It is important to distinguish metal carbides in natural and HPHT synthetic Ila diamonds when there are no crystalline mineral inclusions. Thus, the morphology and Raman spectroscopy of inclusions in Ila diamonds are useful indicators.

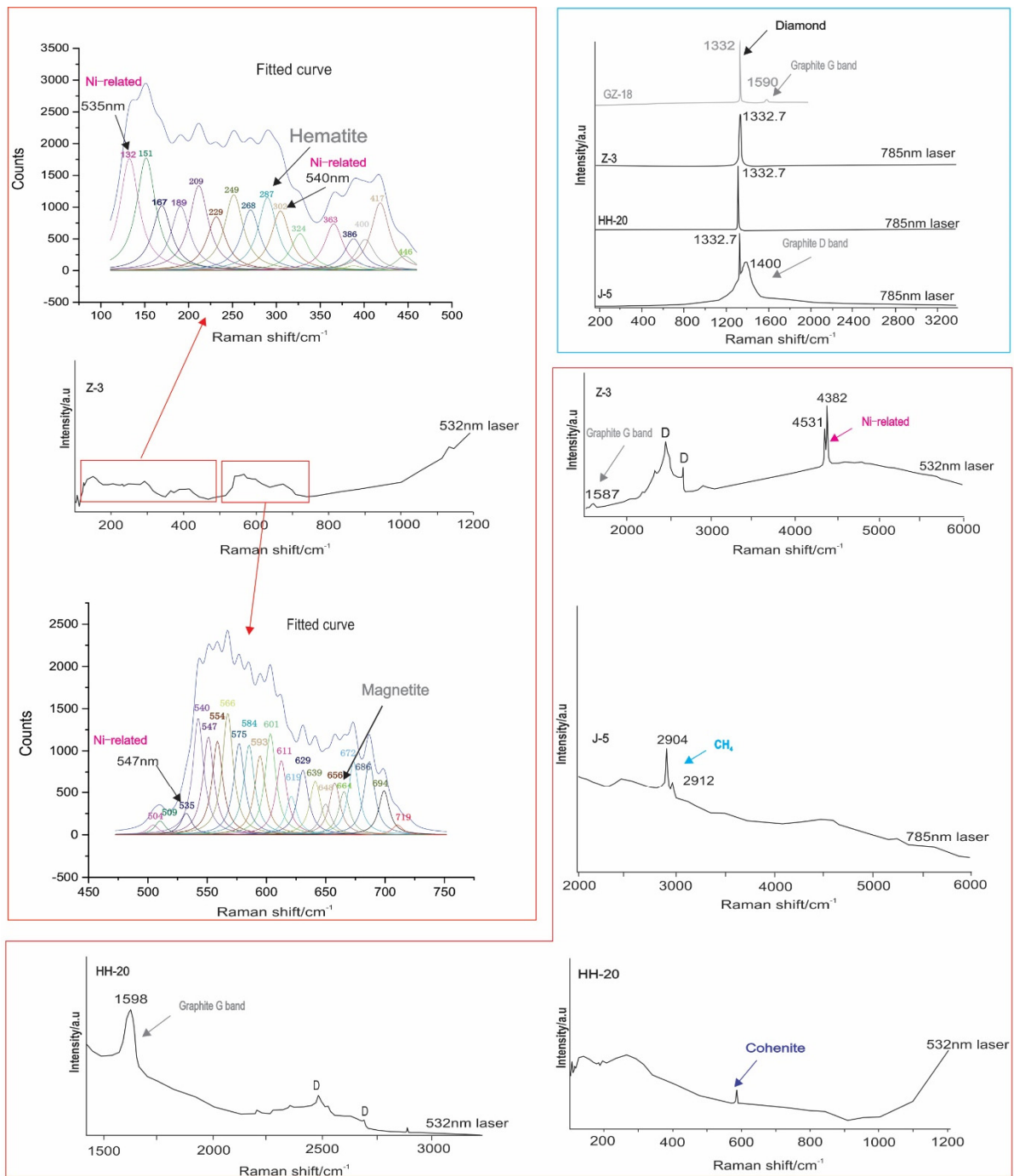


Figure 4. Raman spectroscopy of diamonds and inclusions in Chinese HPHT synthetic diamonds. **The red frame:** Raman Spectroscopy of inclusions in Chinese HPHT synthetic diamond. In sample Z-3, lichenoid inclusions demonstrated complex Raman and electron emission peaks; two red arrows point to the fit and division of the sample Z-3 original Raman lichenoid inclusions. The Cohenite in sample HH-20 are coated with graphite, which is often observed in our HPHT samples. Sample J-5 contains methane gas inclusions encircling metal alloys. Diamond Raman features are marked “D”. **The blue frame:** Raman spectroscopy of samples.

Table 2. Summary of inclusions observed in type IIa colorless diamonds.

No. of Diamonds	Color/Style	Largest in Group	Inclusion Assemblage	Inclusion Properties	Origin	Delivery Time/Reference
11	Colorless /IIa	1.02ct	Undetected, metal alloy, carbide, and containing complicated emission peaks.	Tiny point-like inclusions, silver/black color transparent to opaque, less than 1 μm . Rod-like, pear, water-drop inclusions along with four angles at the end of <111> chains, 4 also had graphite + CH ₄ jacket (did not have detectable H ₂ in Raman). Lichenoid (tree-like) inclusion tubular (cone like), kite-like inclusion along face {100} margin.	HH,J,Z	2018–2020
3	Colorless /IIa	0.17ct	Undetected.	Graphite.	Guizhou of China	2020
60	Colorless /IIa	30.13ct	Crystal minerals, metallic Fe-Ni-C-S (inferred to be primary melt inclusions).	Perovskite, walstromite, majoritic garnet, titanite, larnite, magnetic, silver/black color, opaque, grouped in <111> chains, CH ₄ fluid jacket (22 also had detectable H ₂ in Raman); associated with healed cracks; altered to red-brown (hematite).	South Africa	Smith et al., 2016, 2017
1	Colorless /IaB	Almost 0.80ct	Metal alloy, metallic compound.	-	Brazil	Kaminsky et al., 2011

3.3. PL Spectroscopy and Mapping

For testing purposes, we directionally sectioned the synthetic samples in this study. There was a smooth plane thrown out for the sample without a crystal row in the Guizhou diamond samples. Diamond inclusions are invisible microscopic defects that can reflect the conditions under which diamonds are formed. The position of PL peaks is often used to identify diamonds. HH, J and Z factory HPHT diamonds (total eight grains) had peaks at 693, 694, 883 and 884 nm, which were attributed to an interstitial Ni⁺ atom that was distorted [16,17]. As shown in Figure 5, sample Z-3 exhibited an emission multiplet with lines at 484 nm (2.56 eV), which was Ni-related. The negatively charged silicon-vacancy doublet (SiV⁻, 737 nm, 1.68 eV) was only detected for J factory in four of the samples. We did not observe some PL peaks features which were previously observed in products of ZhongNan (peaks at 494, 503, 658 nm) [18], Power (489 nm) [2] and ZhongWu (peaks at 450, 659, 670, 707 and 714 nm) [19] which were HPHT diamonds factories of China. The peaks at 406, 612, 676, 710, 741, 745 and 945 nm were only observed in the Guizhou natural type IIa diamonds. We found that the greater the number of inclusions, the more impurity defect peaks there were. For more details, see Table 1 and Figure 5.

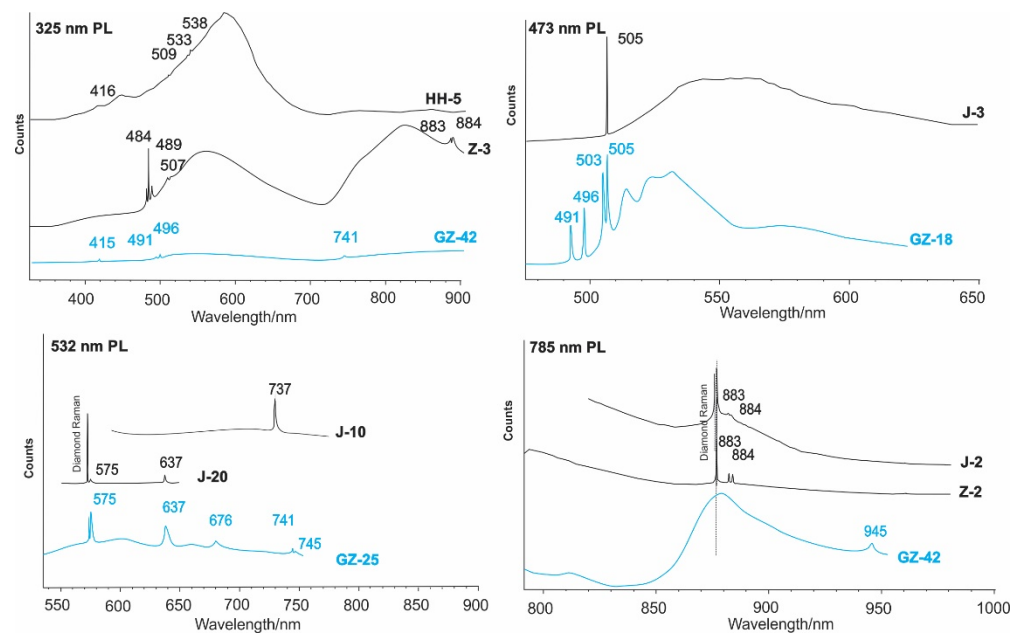


Figure 5. PL Spectroscopy of typical samples (GZ samples in blue color, HPHT samples in black color).

Previous studies indicated which PL peaks are unique to natural diamonds and which are unique to synthetic diamonds [16]. However, with the improvement of HPHT type IIa synthesis technology, impurity defects are decreasing. Some only appeared at 505 and 637 peak positions, or only showed the same PL peaks (693, 694, 737, 883 and 884 nm) as natural diamonds. In this study, both the HPHT and the Guizhou IIa diamonds possessed the H_3 , NV^0 and NV^- centers with peaks at 505, 575 and 637 nm, respectively. Additionally, a 737 nm peak (SiV^-) was found in both the HPHT and natural samples [2,20]. Additionally, PL peaks at 693 and 694 nm were found in synthetic diamonds from IIa HPHT in AOTC [17], as well as natural ultra-deep mantle diamonds [21]. Prior studies distinguished between natural and synthetic colorless diamonds by different types (Ia, Ib, IIa) of diamonds, mineral inclusions, fluorescence and spectral characteristics caused by defects from impurities entering the crystal lattice [22]. Similar impurity defects (fluorescence and spectral characteristics) make it increasingly difficult to distinguish between colorless HPHT synthetic and natural diamonds.

We performed PL mapping at the same peak position in HPHT and natural diamonds, with the aim of distinguishing between them. We mapped each sample using a smooth plane's PL, with peak area distribution peaks at 637, 575 and 496 nm. Figure 6 demonstrates the typical samples. HPHT synthetics have an interior morphological structure quite different from that of naturally grown IIa diamonds according to PL mapping (637 nm). An HPHT IIa diamond revealed growth sector distribution, whereas natural diamonds had multiple lines and a cloud-like growth morphology. This underlying mechanism was also useful in studying the difference between HPHT-grown and Natural IIa diamonds during PL mapping (Figure 6A,C). The PL peak intensity is essential for this method; otherwise it is ineffective.

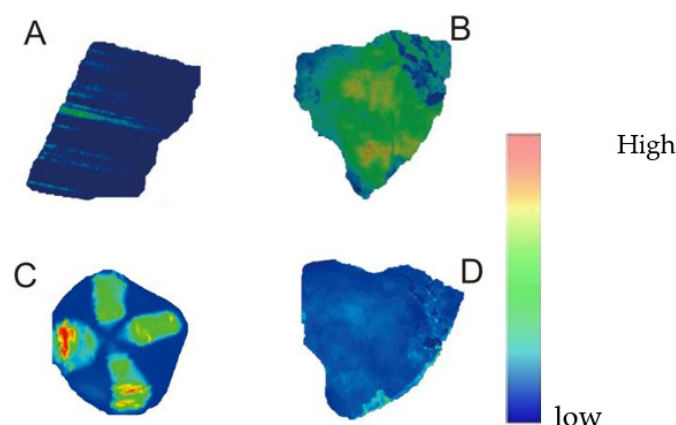


Figure 6. PL mapping images of samples. The baseline-corrected peak area intensity for each laser excitation wavelength. (A) Sample GZ-25, the peak area distribution of the 637 nm peak (532 nm excitation). (B) Sample GZ-42, the peak area distribution of the 575 nm peak (455 nm excitation). (C) Sample J-2, The peak area distribution of the 637 nm peak (532 nm excitation). (D) Sample GZ-42, The peak area distribution of the 496 nm peak (455 nm excitation).

3.4. Chemical Composition of Inclusions

Solvents and catalysts were added to decrease the pressure and temperature of Chinese synthetic HPHT diamonds. Among the Chinese catalysts used are the Ni-Mn-Co, Fe-Al Fe-Ni, Fe-Ni-Si, Fe, Fe-S, Fe-Ni-Co, Ni-Mn-Co-Si, and Fe-Ni-B systems that include metal -Fe, Co, Mn, Al, Ni, Pt, Ru, Rh, Pd, Ir, Os, Ta and Cr- and non-metal-N, and B [1,3]. Catalyst materials can cause inclusions in samples. Aside from catalysts, pressure transmitting media and solvents also contribute to HPHT diamond inclusions [1]. As previously found, the inclusions in HPHT diamonds have mainly solid mineral and gas inclusions including graphite, magnetite, carbide Fe_3C , $(\text{FeNi})_{23}\text{C}_6$, NiC, FeSi_2 , FeNi, FeS, SiC, native metals (e.g., F, Co, Ni, Mn); trace elements (e.g., Ca, Al, Si, S, Cr, Cu, Na, Cl, K, Na, Ti, Mg, P, B, and N) and CH_4 and H_2 (gases) [3,11,23,24]. There is evidence that various elements (N, B, H, O, Ni, Co, S, Ti, P, Si, Ge and Sn, etc) can enter the diamond crystal lattice. Nevertheless, Fe_3C and $(\text{Fe, Ni})_3\text{C}$ carbide inclusions were also found in type IIa super-deep diamonds from Juina Rio Soriso, Brazil; Fe-Ni alloy, Fe-alloy and pyrrhotite also occur in these diamonds. [13–15]. Metallic Fe-Ni-C-S melt systems in natural diamonds have been described previously [14].

For inclusions protruding from diamond faces, we performed a chemical analysis with LA-ICP-MS. Using four colorless typical samples, we tested their inclusions, resulting in 26 points of data. The chemical compositions are shown in the Appendix A, with major elements of Fe-Co-Ni and Co-Mn-Ni distributions (see Figure 7), and different products shown as blue, green and gray balls, respectively, in Chinese gem-quality HPHT IIa diamonds. Trace elements in inclusions in HPHT diamonds include B, Ti, Cu, Zn, Ca, S, P, Cr, etc. (see Appendix A).

A previous study demonstrated that Ni, Mn and Co are the predominant elements in Chinese small abrasive diamond inclusion samples (50–250 m) [24]. The Ni content in inclusions of type Ib small abrasive diamonds has obvious advantages. Iron-carbide inclusions in deep-mantle IIa natural diamonds mainly contain Fe elements, as well as small amounts of Ni and lack Co and Mn [15]. The elements B, Ti and Cu are found in colorless HPHT diamonds at a higher quantity than in yellow diamonds. In recent years, Fe-Co and Fe-Co-Ni systems have been mainly used in Chinese colorless HPHT diamonds; B, Ti and Cu may be nitrogen collectors in HPHT diamonds. We compared the composition of the carbide inclusions in natural diamonds and synthetic diamonds. The major difference between natural and synthetic diamonds is the absence of Co and Mn elements in the natural carbide inclusions. Carbide inclusions in natural diamonds were rare and little information was available about them. Ideally, more trace elements from

natural I₂a diamond carbide inclusions should be examined in the future to compare the differences between HPHT diamonds and natural I₂a diamonds.

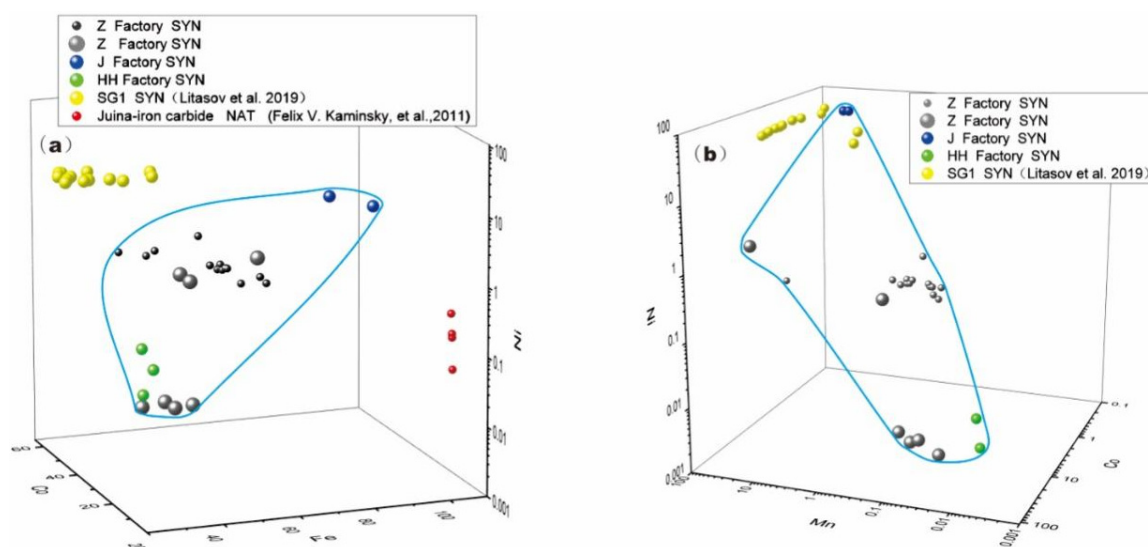


Figure 7. (a) Fe–Co–Ni, (b) Co–Mn–Ni elements plots in inclusions of diamonds, data did normalization operation. Sample numbers are HH-5, HH-20, Z-1, Z-3, J-3 in this study; SG1 are yellow abrasive diamonds, data from Litasov et al. [24]; Julia-iron carbide is a natural super deep diamond, data from Kaminsky et al. [15]; SYN- Synthetic diamond, NAT- Natural diamond; colorless HPHT diamonds characteristics in the blue circle.

4. Conclusions

This study indicates that it is difficult to identify colorless type I₂a diamonds, but some details can provide support. The main conclusions are as follows:

- (1) Finding characteristic inclusions and testing their Raman spectra to identify I₂a diamonds is useful. Different manufacturers have different inclusions in their products due to their different techniques. The kite-like and lichenoid inclusion were not found in natural diamonds, and the abnormal electronic activity characteristics of the lichenoid (tree-like) inclusions in the range of the Raman shift wave-number of 100 to 750 cm^{-1} were clearly different from those of natural diamond inclusions. Furthermore, the HPHT samples did not have healed cracks around the inclusions. Stress differences were also observed around inclusions.
- (2) There were no I₂a diamonds with characteristic inclusions or Raman spectra of inclusions. PL spectroscopy and mapping can provide evidence for identification. We observed peaks only in Guizhou natural type I₂a diamonds at 406 nm, 612 nm, 676 nm, 710 nm, 741 nm, 745 nm and 945 nm. These peaks are missing in HPHT diamonds. The I₂a diamond growth environments can be determined by performing particular peak position PL mapping, such as at 503, 505, 694 and 737 nm. These peaks were found in both natural and synthetic HPHT I₂a diamonds. HPHT I₂a colorless diamond PL mapping revealed the outlines of the growth sectors, whereas natural I₂a colorless diamonds had a line and cloud-like growth morphology.
- (3) The chemical composition of the iron-carbide inclusion in samples where the inclusion was exposed helped to effectively distinguish HPHT from natural I₂a colorless diamonds. The iron carbide inclusions of natural I₂a diamonds are not dominated by Co and Mn elements. Trace elements in inclusions in HPHT I₂a diamonds include B, Ti, Cu, Zn, Ga, Se, S, P and Zr, etc. We still need more natural samples for comparison of the trace elements in inclusions in natural I₂a diamonds.

Thus, the morphology of inclusions and complex Raman spectroscopy of lichenoid (tree-like) inclusion, PL perks, particular peak position PL mapping and the chemical

composition of the iron-carbide inclusion can help to distinguish natural diamonds from HPHT Iia colorless diamonds. These tests provided more information than can be determined from a DiamondView image, IR and PL alone. However, for diamonds with no characteristic inclusions and no PL peaks, we suggest that other images such as CL images and X-ray images (XRT) are needed for further analysis.

Author Contributions: Conceptualization, Y.M. and Z.Q.; data curation, Z.S. and T.L.; formal analysis, Y.M.; funding acquisition, X.D. and Z.Q.; investigation, Y.M., T.D., Z.S. and H.L.; methodology, Y.M. and Z.Q.; software, Y.M.; supervision, T.D., H.L. and Z.S.; validation, Y.M., J.W. and W.Z.; visualization, Y.M.; writing—original draft, Y.M.; writing—review and editing, Y.M. and Z.Q. All authors have read and agreed to the published version of the manuscript.

Funding: This research was funded by NSFC (Nos. 41473030 and 42073008).

Institutional Review Board Statement: Not applicable.

Informed Consent Statement: Not applicable.

Data Availability Statement: Not applicable.

Acknowledgments: Thanks to General Manager Weizhang Liang of the Guangzhou Diamond Exchange; and Jianguo Liu, Jingru Shao and Dufu Wang for arranging our factory visits during 2017–2020. The authors also thank anonymous contributors for generously donating diamond samples, and the analysts at the Shandong Bureau of China Metallurgical Geology Bureau. We also would like to thank Thiering Gerg and J.W. Harris for their assistance during the writing process.

Conflicts of Interest: The authors declare no conflict of interest.

Appendix A

Table A1. Trace element compositions of the inclusions in HPHT diamonds.

sample No.	Spot	Elements (10 ⁶)																
		Fe	Co	Ni	Cu	Zn	B	Na	Mg	Al	Si	P	S	K	Ca	Ti	Cr	Mn
ZN-1	1.00	15722.95	9207.83	108.49	26.49	0.00	394.11	381.85	1966.25	15671.47	0.00	0.00	0.00	1.35	0.00	13488.73	79.33	120.71
ZN-1	2.00	425245.97	286763.11	4462.69	20.33	788.07	290.37	2420.00	251.68	3602.65	2810.52	411.33	899.71	92.24	1289.13	10142.57	112.75	153.15
ZN-1	3.00	341126.35	377834.59	5927.05	38.86	1.87	25.48	19.08	5.00	4584.04	288.80	85.46	8303.31	0.00	0.00	6204.30	44.40	135.64
ZN-1	4.00	291955.62	424632.93	4562.00	28.97	5.16	23.45	157.12	6.52	3330.97	1070.61	77.55	1755.68	74.89	343.42	2248.54	69.26	95.17
ZN-1	5.00	330289.86	390259.89	4744.13	56.04	2.78	48.67	93.10	8.55	3453.61	142.42	34.71	5031.86	2669.60	15012.94	114.91	79.94	200.56
ZN-1	6.00	409077.40	280794.83	4556.43	104.72	4.79	36.90	56.30	7.69	4459.46	2166.45	0.00	0.00	99.95	0.00	2268.67	71.89	66.16
ZN-1	7.00	382435.64	267411.61	4029.91	80.42	30.10	25.11	0.00	4.17	4440.86	29777.87	860.26	736.29	951.93	2758.90	152.41	29.57	35.83
ZN-1	8.00	391707.73	289360.44	4642.30	44.61	19.01	0.00	207.25	0.00	5016.74	10301.09	0.00	0.00	487.78	3691.14	56.73	83.79	89.96
ZN-1	9.00	481099.98	241767.23	4394.33	145.88	12.88	24.14	33.97	2.97	3198.08	0.00	139.19	0.00	0.00	2466.27	63.16	131.61	
ZN-1	10.00	410618.62	266586.04	4561.86	1601.21	1411.06	621.52	4226.40	474.80	6262.01	7084.22	889.36	18713.37	3010.27	6400.09	678.71	72.46	117.90
ZN-1	11.00	434109.29	285879.80	4851.82	30.98	29.43	7.60	0.00	3.62	5306.09	0.00	0.00	13579.38	1026.45	3227.97	52104.71	243.05	120.62
ZN-1	12.00	490450.56	234721.96	3678.41	6.69	619.85	290.80	1805.92	123.16	2383.57	0.00	374.05	1128.02	1369.91	7710.53	4815.41	380.84	177.24
ZN-1	13.00	391844.93	312419.35	12586.81	0.58	620.44	341.90	1333.56	74.66	4571.32	3532.20	127.67	12730.19	1017.74	8485.03	2862.41	575.06	127.13
ZN-1	14.00	410179.80	280336.94	5130.10	78.26	16.46	67.23	186.02	0.00	3143.57	19452.95	0.00	2964.44	223.43	0.00	20678.02	115.93	59.14
ZN-3	1.00	45.37	457987.59	82.56	41447.08	1523.03	9.02	9932.21	405.97	839.12	0.00	258.25	6953.02	368.32	11470.27	15764.10	110.60	76.28
ZN-3	2.00	45.42	387428.42	47.74	17763.66	361.22	26.02	3131.49	127.86	227.71	8746.18	176.40	1434.60	84.70	0.00	49078.02	115.25	38.96
ZN-3	3.00	456165.76	386714.29	44.72	8026.88	22.06	0.00	6.67	6.85	33.41	0.00	6.30	0.00	145.28	0.00	8970.77	189.59	231.03
ZN-3	4.00	399980.98	416146.11	40.30	16723.89	119.14	0.00	176.86	21.09	83.83	0.00	0.00	133.98	521.82	25865.94	170.90	126.48	
ZN-3	5.00	9233.82	7923.87	59.51	22.75	170.02	151.06	404.78	506.06	67122.66	58993.98	1585.44	68812.65	521.35	15524.74	324081.21	47.50	0.00
ZN-3	6.00	2459.78	1252.57	42.94	14.12	72.01	0.00	245.86	803.56	44053.01	55168.43	0.00	172330.18	0.00	0.00	314811.22	26.95	155.53
ZN-3	7.00	29238.30	26965.70	236.74	33.95	134.33	270.57	602.76	3947.10	99557.17	69705.19	2614.04	139507.44	542.01	0.00	359955.68	71.55	28.15
J-3	1.00	1.74	62.18	3197.96	198.82	217.77	82.84	17799.33	13361.19	926027.11	390.98	583.16	16541.57	697.62	77.01	41315.53	178.52	89.63
J-3	2.00	0.56	38.87	2039.09	126.91	519.46	133.02	7544.77	8564.33	939312.41	3336.38	866.11	0.00	0.00	0.00	9.89	55.04	401.05
HH-5	1.00	50.13	424225.41	76.74	22537.87	55.22	16.20	374.55	19.49	279.83	0.00	183.52	0.00	129.67	0.00	0.00	55.81	444.76
HH-5	2.00	56.85	356434.84	88.11	26616.94	195.71	11.94	597.58	223.01	276.97	0.00	93.25	780.53	25.88	0.00	0.00	41.84	419.09
HH-20	1.00	44.54	438244.96	96.49	14054.54	77.61	13.53	293.56	34.53	144.00	338.60	0.00	12908.53	2285.82	15461.07	90.48	37.04	366.48
HH-20	2.00	52.17	366766.51	55.21	16184.89	284.54	0.00	2081.87	171.15	817.33	316.45	0.00	2740.80	3044.31	1998.53	353.62	49.51	408.98

References

- Luo, X.Y.; Xu, Y.J.; Liu, Y.B. The development and key technological improvement of synthetic diamond in China. *Powder Metall. Ind.* **2016**, *26*, 1–13.
- Song, Z.H.; Lu, T.J.; Ke, J.; Su, J.; Tang, S.; Gao, B.; Hu, N.; Zhang, J.; Wang, D.F. Identification characteristic of large near-colorless HPHT synthetic diamond from China. *J. Gems Gemmol.* **2016**, *18*, 1–8.
- Lu, T.; Ke, J.; Lan, Y.; Song, Z.; Zhang, J.; Tang, S.; Su, J.; Dai, H.; Wu, X. Current Status of Chinese Synthetic Diamonds. *J. Gemmol.* **2019**, *36*, 748–757. [[CrossRef](#)]
- Choi, H.; Kim, Y.; Seok, J. Recent trends of gem-quality colorless synthetic diamonds. *J. Korean Cryst. Growth Cryst. Technol.* **2017**, *27*, 149–153.
- He, X.; Du, M.; Zhang, Y.; Chu, P.K.; Guo, Q. Gemology and Spectroscopy Properties of Chinese High-Pressure High-Temperature Synthetic Diamond. *JOM* **2019**, *71*, 2531–2540. [[CrossRef](#)]

6. Welbourn, C.M.; Cooper, M.; Spear, P.M. De Beers Natural versus Synthetic Diamond Verification Instruments. *Gems Gemol.* **1996**, *32*, 156–169. [[CrossRef](#)]
7. Breeding, C.M.; Shen, A.H.; Eaton-Magaña, S.; Rossman, G.R.; Shigley, J.E.; Gilbertson, A. Developments in Gemstone Analysis Techniques and Instrumentation During the 2000s. *Gems Gemol.* **2010**, *46*, 241–257. [[CrossRef](#)]
8. Meng, Y.F.; Peng, M.S.; Wang, J.Y.; Huang, W.X.; Yuan, Q.X.; Zhu, P.P. Monochromatic X-ray topography of diamonds with synchrotron radiation. *Acta Mineral. Sin.* **2005**, *25*, 353–356.
9. Shiryaev, A.A.; Zolotov, D.A.; Suprun, O.M.; Ivakhnenko, S.A.; Averin, A.A.; Buzmakov, A.V.; Lysakovskiy, V.V.; Dyachkova, I.G.; Asadchikov, V.E. Unusual types of extended defects in synthetic high pressure—High temperature diamonds. *Cryst. Eng. Comm.* **2018**, *20*, 7700–7705. [[CrossRef](#)]
10. Muiyal, J. Lab Notes: Cleavage System in Pink Diamond. *Gems Gemol.* **2015**, *51*, 324–325.
11. Frezzotti, M.L.; Tecce, F.; Casagli, A. Raman spectroscopy for fluid inclusion analysis. *J. Geochem. Explor.* **2012**, *112*, 1–20. [[CrossRef](#)]
12. Smith, E.M.; Wang, W. Fluid CH₄ and H₂ trapped around metallic inclusions in HPHT synthetic diamond. *Diam. Relat. Mater.* **2016**, *68*, 10–12. [[CrossRef](#)]
13. Smith, E.M.; Shirey, S.B.; Wang, W. The Very Deep Origin of the World’s Biggest Diamonds. *Gems Gemol.* **2017**, *53*, 388–403. [[CrossRef](#)]
14. Smith, E.M.; Shirey, S.B.; Nestola, F.; Bullock, E.S.; Wang, J.; Richardson, S.H.; Wang, W. Large gem diamonds from metallic liquid in Earth’s deep mantle. *Science* **2016**, *354*, 1403–1405. [[CrossRef](#)] [[PubMed](#)]
15. Kaminsky, F.V.; Wirth, R. Iron Carbide Inclusions In Lower-Mantle Diamond From Juina, Brazil. *Can. Mineral.* **2011**, *49*, 555–572. [[CrossRef](#)]
16. Zaitsev, A.M. *Optical Properties of Diamond: A Data Handbook*; Springer: Berlin/Heidelberg, Germany; New York, NY, USA, 2001; pp. 48–275.
17. D’Haenens-Johansson, U.F.; Moe, K.S.; Johnson, P.; Wong, S.Y.; Lu, R.; Wang, W. Near-Colorless HPHT Synthetic Diamonds from AOTC Group. *Gems Gemol.* **2014**, *50*, 30–45. [[CrossRef](#)]
18. Tang, S.; Lu, T.J.; Song, Z.H.; Ke, J.; Zhang, J.; Zhang, J.; Liu, Q.K. Gemological properties and identification of ZhongNan Gem-quality HPHT diamonds. *China Gems* **2017**, *1*, 212–215.
19. Liang, R.; Lan, Y.; Zhang, T.Y.; Lu, T.J.; Chen, M.Y.; Wang, X.Q.; Zhang, X.H. Multi-spectroscopy studies on large grained HPHT synthetic diamonds from Shandong, China. *Spectrosc. Spectr. Anal.* **2019**, *39*, 1840–1845.
20. Breeding, C.M.; Wang, W. Occurrence of the Si-V defect center in natural colorless gem diamonds. *Diam. Relat. Mater.* **2008**, *17*, 1335–1344. [[CrossRef](#)]
21. Ma, Y.; Li, H.H.; Zhu, X.X.; Ding, T.; Lu, T.J.; Qiu, Z.L. Lab Notes: D color natural Iia diamond with the walstromite inclusion. *Gems Gemol.* **2018**, *4*, 241–243.
22. Breeding, C.M.; Shigley, J.E. The “Type” Classification System of Diamonds and Its Importance in Gemology. *Gems Gemol.* **2009**, *45*, 96–111. [[CrossRef](#)]
23. Guo, M.-M.; Li, S.-S.; Feng, L.; Hu, M.-H.; Su, T.-C.; Gao, G.-J.; Wang, J.-Z.; You, Y.; Nie, Y. The effect of adding Cu on the nitrogen removal efficiency of Ti for the synthesis of a large type Iia diamond under high temperature and high pressure. *New Carbon Mater.* **2020**, *35*, 559–566. [[CrossRef](#)]
24. Litasov, K.D.; Kagi, H.; Bekker, T.B.; Hirata, T.; Makino, Y. Cuboctahedral type Ib diamonds in ophiolitic chromitites and peridotites: The evidence for anthropogenic contamination. *High Press. Res.* **2019**, *39*, 480–488. [[CrossRef](#)]